Rev.Adv.Mater.Sci. 19 (2009) 63-72

GENERATION AND CONVERENCE OF NANOCRACKS IN NANOCRYSTALLINE MATERIALS DEFORMED BY GRAIN BOUNDARY SLIDING

N.F. Morozov[1,2], I.A. Ovid'ko[1,2], Yu.V. Petrov[1,2] and A.G. Sheinerman[2]

[1]Research Institute for Mathematics and Mechanics, St. Petersburg State University, Universitetskii 28, Stary Petergof, St. Petersburg 198504, Russia
[2]Institute for Problems of Mechanical Engineering, Russian Academy of Sciences, Bolshoj 61, Vasil. Ostrov, St. Petersburg 199178, Russia

Received: December 03, 2008

Abstract. A theoretical model is suggested which describes the generation of nanocracks at grain boundaries and their convergence into a catastrophic macrocrack in nanocrystalline materials deformed by grain boundary sliding. The criterion for the convergence is revealed, and the fracture strength of a nanocrystalline material is calculated which characterizes the formation of a catastrophic macrocrack due to the convergence. Also, we estimated strain-to-failure controlled by grain boundary sliding, generation of nanocracks and their convergence. It is shown that both the fracture strength and strain-to-failure of a nanocrystalline material deformed through grain boundary sliding are highly sensitive to the misorientation angles of grain boundaries that dominate in the material.

1. INTRODUCTION

Nanocrystalline materials – solids consisting of nanoscale grains (crystallites with the sizes below 100 nm) divided by interfaces (grain and interphase boundaries) – represent the subject of intensive research in various branches of science, including solid state mechanics. Nanocrystalline materials show outstanding mechanical properties attributed to their structural features, first of all, nanoscale sizes of crystallites and large amounts of interfaces (grain and interphase boundaries); see, e.g., reviews [1–7] and books [8,9]. In this context, mechanics of nanocrystalline materials should definitely involve in a detailed consideration their structure and its evolution under a mechanical load. In particular, it is effective to exploit the sinergetic approach in mechanics of nanocrystalline materials. This approach focuses on evolution of both the nanostructure and structural defects in mechanically loaded nanocrystalline specimens, in parallel with an analysis of stresses and their relaxation through plastic deformation and fracture processes associated with the evolution. The sinergetic approach represents a modification/generalization of classical mechanics [10–13] of conventional polycrystalline solids under a mechanical load. In fact, this approach involves representations of classical mechanics, solid state physics and materials science.

Of particular importance for mechanics of nanocrystalline materials and their structural applications are the strength and ductility of these mate-

Corresponding author: I.A. Ovid'ko, e-mail: ovidko@def.ipme.ru

rials. The ultimate strength of nanocrystalline materials is commonly 2–10 times higher than that of conventional polycrystals with the same chemical composition [1-9]. At the same time, for most of nanocrystalline materials, tensile strain-to-failure ε_f does not exceed several per cent (ε_f=0.02-0.03) [1–9]. Low ductility of nanocrystalline solids (characterized by small values of ε_f) considerably limits practical applications of these high-strength materials. At the same time, there are examples of nanocrystalline solids showing good ductility ($\varepsilon_f \geq 0.08$) in parallel with ultrahigh strength [14–21]. Besides, some nanocrystalline metals and ceramics demonstrate a superplastic behavior (ε_f>2) at lower temperatures and higher strain rates compared to their polycrystalline counteparts [22–27]. The nature of ductility and superplasticity of nanocrystalline solids is the subject of wide speculations (see, e.g., [1–9]). At the same time, there are no doubts in the fact that ductility of nanocrystalline solids is highly sensitive to their structural features causing the actions of the specific mechanisms of their plastic deformation and fracture. In these circumstances, the identification of these mechanisms (which, generally speaking, are different from those operating in conventional polycrystalline materials) is crucially important for the progress in fabrication of nanocrystalline materials with simultaneously ultrahigh strength and good ductility.

In this context, one of the key problems of nanomaterials mechanics is an adequate theoretical description of the processes of nanoscale fracture and the mechanisms responsible for the transition from nanoscale to macroscale fracture. One treats that such mechanisms are different in nanocrystalline and conventional polycrystalline materials due to the difference in the structure between these materials (see, e.g., experimental data [16,19–21,28–31], computer models [32–35] and theoretical studies [36–43]). In particular, brittle fracture of nanocrystalline metals with the face-centered cubic crystal lattice (fcc metals) has been observed in experiments [29–31]. At the same time, brittle fracture of conventional polycrystalline fcc metals under a quasistatic load is not typical. The specific features of fracture processes of nanocrystalline materials are first of all governed by their structural peculiarities, namely the nanoscopic dimensions of their grains and the very high volume fractions occupied by grain boundaries (GBs); for a review, see [44]. In theoretical papers [36,37], the experimentally observed brittle fracture of nanocrystalline solids was attributed to the catastrophic convergence of nanocracks. These studies were mainly focused on the derivation of the conditions for the convergence of the existing nanocracks, whereas the processes of nanocrack nucleation were not analyzed, and the estimate of the fracture strength σ_B and strain-to-failure ε_f was not made. The main aim of this paper is to elaborate a detailed model describing multiple generation of nanocracks and their catastrophic convergence in deformed nanocrystalline materials. Within the model, we examine nanocrack generation in the course of GB sliding (one of the dominant modes of (super)plastic deformation in nanocrystalline materials) and estimate both the fracture strength σ_B and strain-to-failure ε_f.

2. MODEL

The nucleation and growth of a crack in a solid commonly occurs under the action of both the applied stress and the stress fields created by defects, the sources of internal stresses. Such defects can either be present in a solid prior to its mechanical loading or be created during its plastic deformation. In general, several mechanisms of plastic deformation are active in nanocrystalline materials [1–9], in contrast to the case of polycrystals where the conventional slip of lattice dislocations in grain interiors is dominant. Among various mechanisms of plastic deformation of nanocrystalline materials, one can distinguish GB sliding as the dominant deformation mode under certain conditions. In particular, GB sliding plays the key role in the processes of superplastic deformation of nanocrystalline materials (e.g., [9,24,27]). Also, GB sliding is considered as the dominant or, at least, one of the principle deformation modes in nanocrystalline materials with fines grains (with the size below 15 nm) [1–9], where the volume fraction of GBs – carriers of GB sliding – is particularly high. With the important role of GB sliding in the processes of plastic deformation, we will consider the generation and convergence of nanocracks in nanocrystalline materials with finest grains (d<15 nm), deformed primarily through GB sliding. (According to experimental data [29–31], it is precisely these materials that are particularly prone to brittle fracture.)

In general, nanocrystalline materials can fracture both due to the convergence of pre-existent cracks/voids and as a result of the generation of new nanocracks during plastic deformation. In the following, we will consider nanocrystalline materials without pre-existent cracks and voids. Within the model, we examine two processes: (1) nanoscopic fracture that manifests itself in nanocrack generation at GBs in the course of GB

sliding; and (2) the transition from nanoscopic to macroscopic fracture owing to the convergence of nanocracks in neighboring GBs and the formation of a catastrophic macrocrack.

First, let us consider the generation of nanocracks in nanocrystalline solids during GB sliding. To do so, we examine a nanocrystalline specimen under a tensile applied load $\sigma_{yy}=\sigma$ (Fig. 1). Let this specimen be plastically deformed through GB sliding. In general, GB sliding leads to the formation of two kinds of defects near triple junctions of GBs: dislocations with large Burgers vectors and disclination dipoles [45]. The formation of dislocations is associated with the incompatibility of strains at triple junctions, appearing in the course of GB sliding. When dislocations are accumulated in triple junctions, they induce high local stresses that provide strain hardening and promote nanoscopic fracture. At the same time, dislocations under the action of the applied stress can be emitted from triple junctions into grain interiors. In this case, the dislocations move far from triple junctions and, consequently, do not significantly influence the processes of GB sliding and nanocrack generation. In these circumstances, for simplicity, in the following, we will not account for the effects of dislocations on these processes.

Along with dislocation formation, GB sliding results in the formation of disclination dipoles near triple junctions [42,45]. The formation of disclination dipoles is associated with the displacement of GBs during GB sliding from the triple junctions of GBs to their new positions [42,43]. Every such a disclination dipole comprises a disclination at a triple junction and a second opposite-sign disclination at a GB, and the dipole arm (distance between its disclinations) amounts to the jump of displacements along a GB during GB sliding (Fig. 2b). In the case of tilt boundaries, the disclinations are of wedge character, and the disclination strengths are equal by magnitude to the misorientation angles of the moving boundaries or to the difference of the misorientation angles from $2\pi/m$, where m is the order of the crystal symmetry axis. (For typical fcc nanocrystalline metals, m=4.) Disclination dipoles formed at GBs hinder GB sliding and thereby provide strain hardening of nanocrystalline materials [42].

When the values of the dipole disclination strengths and dipole arms are sufficiently high, disclination stresses can initiate nanocrack generation [43]. Nanocracks nucleate in the nanoscopic regions near disclination cores, where the disclination-induced tensile stresses exceed the local

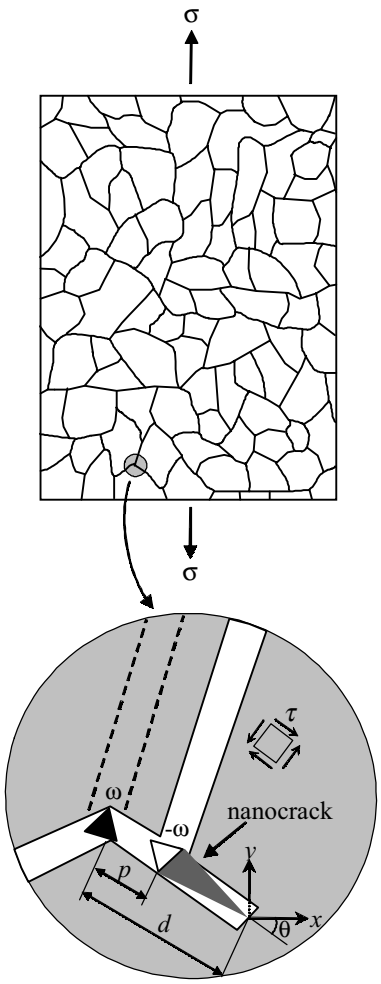

Fig. 1. Nanocrystalline specimen under a one-axis tensile load. The ellipse shows a disclination dipole and nanocrack formed at a grain boundary due to grain boundary sliding.

fracture strength and lead to the formation of free surfaces. Our estimates based on the expressions for the disclination dipole stress fields [46] show that, in the considered case where the grain size d<15 nm, the equilibrium nanocrack lengths are much smaller than the grain size. This inequality is valid even in the situation with very significant sliding along a GB (characterized by the jump of displacements equal to d). At the same time, these nanocracks can serve as nuclei for the formation of larger nanocracks with the size close to the grain size d.

Let us consider the mechanism for the formation of such nanocracks (Fig. 2). Let a disclination dipole form in a GB due to GB sliding (realized under the action of a local shear stress τ) (Figs. 2a

and 2b). Simultaneously, GB sliding results in the formation of a triple junction dislocation which is then emitted into the grain interior (Fig. 2b). When the jump of displacements along a GB due to GB sliding reaches a critical value, a nanocrack is generated at one of the dipole disclinations (Fig. 2c). The subsequent GB sliding results in the shear of the crack surfaces and crack elongation (Figs. 2d and 2e). Then the crack surface becomes smoother (Fig. 2f) owing to diffusion along this surface. (The driving force for the crack surface diffusion is a decrease of the crack surface area leading to a decrease in the crack surface energy.) The following GB sliding leads to the shear of the crack surfaces and crack elongation to the triple junction, as shown in Fig. 2g. Also, the crack can grow to the left, along the rest of the GB, owing to GB diffusion (Fig. 2h) in the stress field of the high local stresses near the crack tip. Hereafter, we will assume that the above mechanism gives rise to the formation of GB nanocracks whose lengths are approximately equal to the jumps of displacements in GBs resulting from GB sliding.

Now let us consider the convergence of nanocracks (generated at GBs due to GB sliding) into a macrocrack. With an account for nanoscopic crack lengths and high angles between the planes of adjacent GBs, we suppose that the formation of a nanocrack in a specified GB does not depend on the formation of nanocracks in other GBs. In these circumstances, the formation of a macrocrack – the carrier of catastrophic fracture – is the result of the independent events of nanocrack formation in various GBs.

With these assumptions, the process of the propagation of cracks along GBs can be described using the mathematical methods of the percolation theory. This theory connects macroscopic processes of different origins in structured systems with the characteristics of their elementary processes and structure geometry [47–50]. Following the percolation theory [47–50], in the case under our consideration, the formation of a macrocrack that goes through the entire solid (that is, the formation of an infinite cluster that consists of GBs containing nanocracks) is possible, if the number fraction of GBs containing nanocracks exceeds a critical value n_c.

Let all GBs have the same length d. We assume that the nanocracks formed independently in neighboring GBs converge, if the length of all such nanocracks is equal d. Thus, the number fraction n of GBs containing nanocracks that can converge with nanocracks in neighboring GBs equals to the

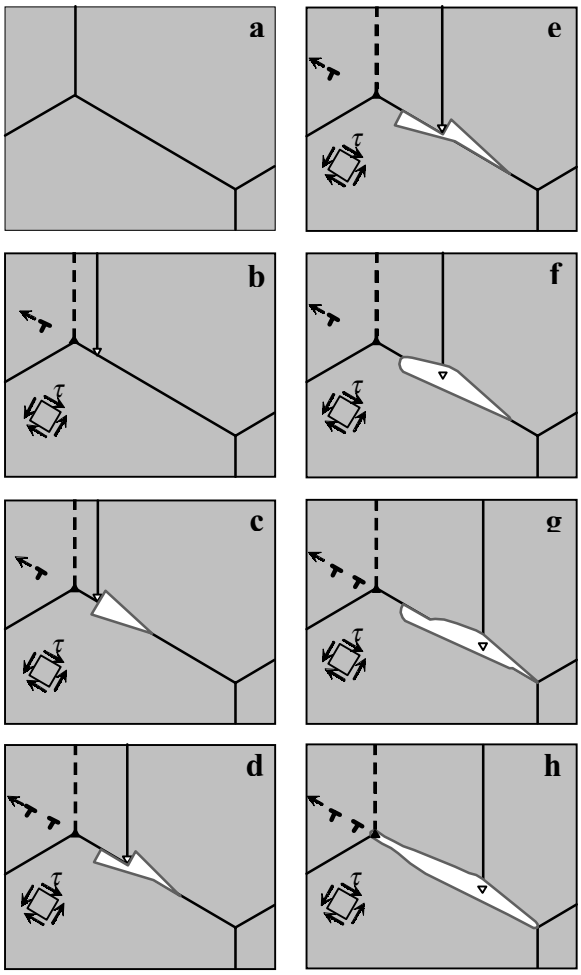

Fig. 2. Formation of a disclination dipole and grain boundary nanocrack as a result of grain boundary sliding in a deformed nanocrystalline material. (a) Initial state of the grain boundary. (b) Disclination dipole is generated in the grain boundary due to grain boundary sliding. Simultaneously, a dislocation forms in a triple junction. Then the dislocation is emitted into the grain interior. (c) Nanocrack generates at one of the dipole disclinations. (d,e) Owing to grain boundary sliding the nanocrack changes its shape and elongates. At the same time, the second dislocation forms in the triple junction. Then the dislocation is also emitted into the grain interior. (f) Nanocrack is smoothen up due to diffusion. (g) Subsequent grain boundary sliding leads to the shear of the crack surfaces and crack elongation to the triple junction. (h) Crack growth to the left, along the rest of the grain boundary, owing to grain boundary diffusion.

number fraction of GBs where the jump of displacements amounts to d.

For estimate of the number fraction n of such GBs we make the following assumptions:

(i) All GBs are tilt boundaries.

(ii) GBs are randomly oriented about the tension axis.

(iii) The jumps of displacements along GBs can vary in the range $o \le p \le d$.

(iv) The jump of displacements along any specified GB does not depend both on the jump of displacements along other GBs and on the angles made by this GB with the neighboring GBs. The jump of displacements along a GB is controlled only by the orientation of this GB with respect to the tension axis and by the strengths of the disclinations formed in this GB in the course of GB sliding.

GBs are specified by a misorientation angle distribution. This distribution produces a distribution of the absolute values of GB disclination strengths that lie in the interval $0 < \omega \le \omega_{max}$.

3. CHARACTERISTICS OF NANOCRACK GENERATION DURING GRAIN BOUNDARY SLIDING

In this section we calculate the condition for the generation of a GB nanocrack of length d. (According to our assumption, such a nanocrack can converge with nanocracks in the neighboring GBs.) Since we suppose that the nanocrack length is equal to the jump of displacements along the GB in the course of GB sliding, the latter condition is equivalent to the relation $p=d$, where p is the jump of displacements, which is also equal to the dipole arm. To calculate the equilibrium value of p, we cast the energy associated with both the GB sliding along an individual GB and the formation of a disclination dipole in this GB. Then the equilibrium value of p will be found from the energy minimum condition.

Let us consider a GB containing a disclination dipole formed due to GB sliding. Let the GB plane make an angle θ with the tension axis, the dipole arm equal to p, and the dipole disclination strengths be equal to ω and $-\omega$ (Fig. 1). In order to estimate the equilibrium dipole arm p, we calculate the energy associated with disclination dipole formation. In so doing, we take into account the fact that the applied tensile load σ creates the shear stress $\tau=(\sigma/2)\sin 2\theta$ in the GB plane (see Fig. 1). The opposite shear stresses create opposite jumps of displacements along the GB. Therefore, without loss of generality, in the following we will examine the GBs for which τ is positive, that is, $0 \le \theta \le \pi/2$.

We assume that along with the shear stress τ which acts in the GB plane and induces GB sliding, there exists an additional internal shear stress in the GB plane, which is not associated with the formation of disclination dipoles. This additional stress characterizes resistance to GB sliding despite the presence or absence of disclination dipoles. We suppose that in the presence of GB sliding, this internal shear stress acting in the GB does not depend on the jump of displacements p along the GB and is equal to τ_f. In this case, for $\tau<\tau_f$, GB sliding along the GB does not occur, while, for $\tau>\tau_f$, an effective shear stress $\tau-\tau_f$ acts in the GB plane. This effective shear stress induces the formation of a disclination dipole in the GB. With this assumption, the energy variation (per unit disclination length) associated with the GB sliding and the formation of a disclination dipole is as follows (see Ref. [42] with the correction made in [51]):

$$\Delta W = \frac{D\omega^2 p^2}{2}\left\{\ln\frac{R}{p}+\frac{3}{2}\right\}-(\tau-\tau_f)pd, \quad \tau > \tau_f, \quad R \ge p. \tag{1}$$

In formula (1), R is the screening length of the disclination dipole stress field, $D=G/[2\pi(1-\nu)]$, G is the shear modulus, and ν is the Poisson's ratio. The first term on the right-hand side of formula (1) describes the disclination dipole self-energy [46], while the second term characterizes the work of the effective shear stress $\tau-\tau_f$ done to provide GB sliding. In formula (1), the interaction between different disclination dipoles is accounted for by the introduction of the screening length R of the disclination dipole stress field. Formula (1) also takes into account that an isolated disclination dipole in an infinite solid does not interact with the constant applied stress.

Assume that the growth of the dipole arm is energetically favored if $\partial\Delta W/\partial p<0$. Then the equilibrium dipole arm is derived from the relation $\partial\Delta W/\partial p=0$, which in combination with formula (1) yields:

$$\tau = \tau_f + \frac{Dp\omega^2}{d}\left(\ln\frac{\kappa d}{p}+1\right). \tag{2}$$

In formula (2), we use the denotation $\kappa=R/d$. Eq. (2) has a solution at $\tau_f \le \tau < \tau_f + D\omega^2\kappa$. If $\tau \le \tau_f$, GB sliding along the GB does not occur ($p=0$), while, for $\tau > \tau_f + D\omega^2\kappa$, GB sliding can go on until it is stopped

by the neighboring triple junctions. We assume that, when $\tau>\tau_f+D\omega^2\kappa$, the jump of displacements along the GB is equal to d ($p=d$). The formation of a disclination dipole with the arm d is energetically favorable provided that the shear stress is not smaller than that necessary to form a disclination dipole with the equilibrium arm d, that is, if

$$\tau \geq \tau_f + D\omega^2(\ln\kappa + 1). \quad (3)$$

For simplicity, we suppose that the stress τ_f acting in a GB does not depend on its misorientation angle. In this case with an increase of the applied stress, GB sliding starts to occur along the favorably oriented GBs making the angles close to $\pi/4$ with the tension axis. As the applied stress σ approaches the yield strength $\sigma=\sigma_y$, the relation $\tau=\tau_f$ should hold in these GBs. Since $\tau=(\sigma/2)\sin2\theta$ and, consequently, $\tau=\sigma/2$ at $\theta=\pi/4$, one obtains that $\tau_f=\sigma_y/2$.

With substitution of the relations $\tau_f=\sigma_y/2$ and $\tau=(\sigma/2)\sin2\theta$ to inequality (3), we rewrite this inequality as $\sin2\theta\geq f(\omega)$, where

$$f(\omega) = \frac{\sigma_y + 2D\omega^2(\ln\kappa + 1)}{\sigma}. \quad (4)$$

The inequality $\sin2\theta\geq f(\omega)$ determines the conditions for the formation of a disclination dipole with the arm d in a GB characterized by the angle θ. As a result, this inequality also determines the condition for the formation of a GB nanocrack that can converge with nanocracks in the neighboring GBs.

4. CRITICAL PARAMETERS FOR CATASTROPHIC CONVERGENCE OF NANOCRACKS IN THE COURSE OF GRAIN BOUNDARY SLIDING

Let us analyze the conditions for the catastrophic convergence of nanocracks in the course of GB sliding in nanocrystalline solids. In order to calculate the number fraction n of GBs containing nanocracks with the length d, following [36,37], we introduce the distributions of GBs over the angles θ and magnitudes ω of disclination strengths. Assume that GBs are randomly oriented and define the distribution density of GBs, $\rho_\theta(\theta)$, over the angles α as $\rho_\theta(\theta)=2/\pi$, where $0\leq\theta\leq\pi/2$. We introduce the denotation $t=\sin2\theta$ and come from the distribution density $\rho_\theta(\theta)$ to the distribution density $\rho_t(t)$. Since, for $0<t<1$, one value of t corresponds to two different values of θ from the interval $0\leq\theta\leq\pi/2$, the distribution density can be presented as

$$\rho_t(t) = \frac{2\rho_\theta(\theta)}{|\,dt/d\theta\,|}(t=\sin2\theta) = \frac{2}{\pi\sqrt{1-t^2}}. \quad (5)$$

Suppose that the absolute values ω of disclination strengths, which vary in the range $0<\omega\leq\omega_{max}$, obey the normalized beta distribution $\rho_\omega(\omega)$:

$$\rho_\omega(\omega) = \frac{(\omega/\omega_{max})^{\alpha-1}(1-\omega/\omega_{max})^{\beta-1}}{\omega_{max}B(\alpha,\beta)}, \quad (6)$$

where α and β are constants, and $B(\alpha,\beta)$ is the beta function. The parameter β is related to the parameter α and the mean value $\overline{\omega}$ of the magnitude ω of disclination strengths as $\beta=\alpha(\omega_{max}/\overline{\omega}-1)$. For a specified $\overline{\omega}$, the parameter α determines the distribution dispersion $\alpha\beta/[(\alpha+\beta)^2(\alpha+\beta+1)]$, which decreases with an increase in α. In the examined case of $\alpha>1$, the distribution density $\rho_\omega(\omega)$ becomes zero at $\omega=0$ or $\omega=\omega_{max}$ and has a single maximum in the range $0<\omega\leq\omega_{max}$.

The number fraction of GBs containing nanocracks that can merge with nanocracks in neighboring GBs is calculated as [52]

$$n = \int_0^{\omega_{max}} \rho_\omega(\omega)P(t>f(\omega))d\omega, \quad (7)$$

where $P(t>f(\omega))$is the probability that $t>f(\omega)$. The probability is given by

$$P(t>f(\omega)) = \Theta(1-f(\omega))\int_{f(\omega)}^{1}\rho_t(t)dt = \frac{2}{\pi}\Theta(1-f(\omega))\arccos f(\omega), \quad (8)$$

where $\Theta(x)$ is the Heaviside function equal to 1 at $x>0$, and to 0 otherwise.

The function $\Theta(1-f(\omega))$ figuring in formula (8) is not equal to 0, if $f(\omega)<1$. The latter relation can be rewritten as $\omega<\omega_c$, where

$$\omega_c = \sqrt{\frac{\sigma-\sigma_y}{2D(\ln\kappa+1)}}. \quad (9)$$

With the inequality and formulas (6) and (8) substituted to formula (7), one obtains the following final expression for the number fraction of GBs containing nanocracks:

$$n = \frac{2}{\pi\omega_{\max} B(\alpha,\beta)} \times \int_0^{\min\{\omega_c,\omega_{\max}\}} \left(\frac{\omega}{\omega_{\max}}\right)^{\alpha-1} \left(1-\frac{\omega}{\omega_{\max}}\right)^{\beta-1} \arccos f(\omega)\, d\omega. \quad (10)$$

Now the criterion of macrocrack formation has the form $n>n_c$, where the critical number n_c of fraction of the GBs "conducting" the nanocracks depends on the grain shape. In the examined case of a nanocrystalline solid, the analysis based on the percolation theory [47–50] gives: $n_c \approx 0.125$.

Formula (10) allows one to relate the number fraction n of the GBs "conducting" the nanocracks with the applied tensile stress σ and to calculate the critical stress $\sigma_c=\sigma(n=n_c)$ for the brittle fracture of the nanocrystalline solid. Another important characteristic of nanocrystalline materials is strain-to-failure ε_f. In the case under our consideration, ε_f is defined as the plastic strain at which a catastrophic macrocrack forms in the nanocrystalline solid: $\varepsilon_f=\varepsilon(n=n_c)$. In order to estimate ε_f, we calculate the dependence of the strain $\varepsilon=\varepsilon_{yy}$ of the nanocrystalline solid on the applied stress σ.

For the calculation of ε, we consider a model two-dimensional nanocrystalline solid consisting of square grains with the side length d, whose boundaries make the angles θ and $\pi/2-\theta$ with the tension axis. Let a dipole of disclinations with the strengths $\pm\omega$ form at every GB and the applied tensile stress induce sliding along every GB characterized by the jump of displacements p. Then sliding along the GBs that make the angle θ with the tensile load direction induces plastic shear by the angle p/d, which, in turn, creates plastic strain $\varepsilon_{yy}^{(1)}=p\sin 2\theta/(2d)$. Sliding along the GBs making the angle with the axis of the applied load also creates plastic shear by the angle and induces plastic strain $\varepsilon_{yy}^{(2)}=\varepsilon_{yy}^{(1)}=p\sin 2\theta/(2d)$. The total strain due to sliding along two families of GBs is equal to $\varepsilon_{yy}^{(1)}+\varepsilon_{yy}^{(2)}$. Using the denotation $t=\sin 2\theta$ and introducing another denotation $\varepsilon(t,\omega)=\varepsilon_{yy}^{(1)}+\varepsilon_{yy}^{(2)}$, we obtain: $\varepsilon(t,\omega)=pt/d$.

As it has been shown above, the jump of displacements p is equal to 0, for $\tau\le\tau_f$; p is calculated from equation (2), for $\tau_f<\tau<\tau_f+D\omega^2(\ln\kappa+1)$ (that is, for $t<f(\omega)$); and p amounts to d at $\tau\ge\tau_f+D\omega^2(\ln\kappa+1)$ (that is, at $t\ge f(\omega)$). With formula (2) as well as the relations $\tau=(\sigma/2)t$, $\tau_f=\sigma_y/2$ and $\varepsilon(t,\omega)=pt/d$, one finds that at $\varepsilon(t,\omega)=0$, $t\le\sigma_y/\sigma$, $\varepsilon(t,\omega)=t$ at $t\ge f(\omega)$, and $\varepsilon(t,\omega)$ is the smallest of the two roots of the equation

$$\frac{\varepsilon(t,\omega)}{t}\left(\ln\frac{\kappa t}{\varepsilon(t,\omega)}+1\right)=\frac{\sigma t-\sigma_y}{2D\omega^2} \quad (11)$$

in the case of $\sigma_y/\sigma<t<f(\omega)$. Solving equation (11) for $\varepsilon(t,\omega)$ and selecting the smallest of its two roots yields:

$$\varepsilon(t,\omega)=\begin{cases}0, & t\le\sigma_y/\sigma\\ \kappa t e^{1+W\left[-(\sigma t-\sigma_y)/2\kappa eD\omega^2\right]}, & \sigma_y/\sigma<t<f(\omega),\\ t, & t\ge f(\omega),\end{cases} \quad (12)$$

where $W(z)$ is the special function defined as the smallest of the two roots of the equation $z=We^W$ in the case of $-1/e<z<0$.

Now let us consider a deformed nanocrystalline solid with randomly oriented GBs and various values ω of disclination strength magnitudes. The average plastic strain $\varepsilon=\varepsilon_{yy}$ in such a solid is found by averaging the strain $\varepsilon(t,\omega)$ over both various GB orientations and disclination strengths ω. The averaging procedure gives:

$$\varepsilon=\int_0^1 \rho_t(t)dt\int_0^{\omega_{\max}}\rho_\omega(\omega)\varepsilon(t,\omega)d\omega= \frac{2}{\pi\omega_{\max}B(\alpha,\beta)}\int_0^1\frac{dt}{\sqrt{1-t^2}}\times \int_0^{\omega_{\max}}\left(\frac{\omega}{\omega_{\max}}\right)^{\alpha-1}\left(1-\frac{\omega}{\omega_{\max}}\right)^{\beta-1}\varepsilon(t,\omega)d\omega. \quad (13)$$

With formulas (4), (10), (12), and (13), we plot the dependences $n(\varepsilon)$ and $n(\sigma)$ in the case of nanocrystalline Ni characterized by the following values of elastic moduli [53]: $G=73$ GPa and $\nu=0.31$. We also put $\kappa=3$, $\omega_{\max}=\pi/4$ and $\sigma_y=0.8$ GPa. The dependences $n(\varepsilon)$ and $n(\sigma)$ are presented in Figs. 3 and 4, respectively, for various values of $\overline{\omega}$ and α. The horizontal lines in these figures show the value of n_c ($n_c\approx 0.125$). The formation of a catastrophic macrocrack is possible in the regions where the curves $n(\varepsilon)$ or $n(\sigma)$ lie higher than the horizontal line $n=n_c$.

As it is seen in Fig. 3a, the curves $n(\varepsilon)$ plotted for different values of the average modulus $\overline{\omega}$ of disclination strength practically coincide, that is, the number fraction n of GBs conducting cracks does not depend on $\overline{\omega}$ at a fixed strain ε. As a consequence, the strain-to-failure ε_f (determined by the point of the intersection of the corresponding curve $n(\varepsilon)$ with the horizontal line $n=n_c$) does not depend

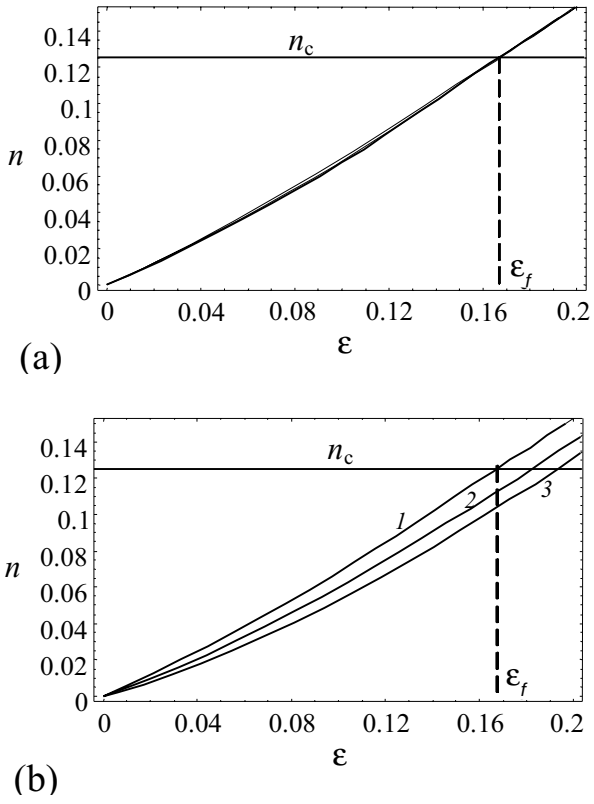

Fig. 3. Dependences of the fraction *n* of the grain boundaries conducting cracks in nanocrystalline Ni on strain ε. (a) α=1.5; $\bar{\omega}$=7, 10 and 15° (the curves corresponding to different $\bar{\omega}$ practically merge). (b) ω=10°; α=1.5, 2 and 2.5 (curves 1, 2 and 3, respectively).

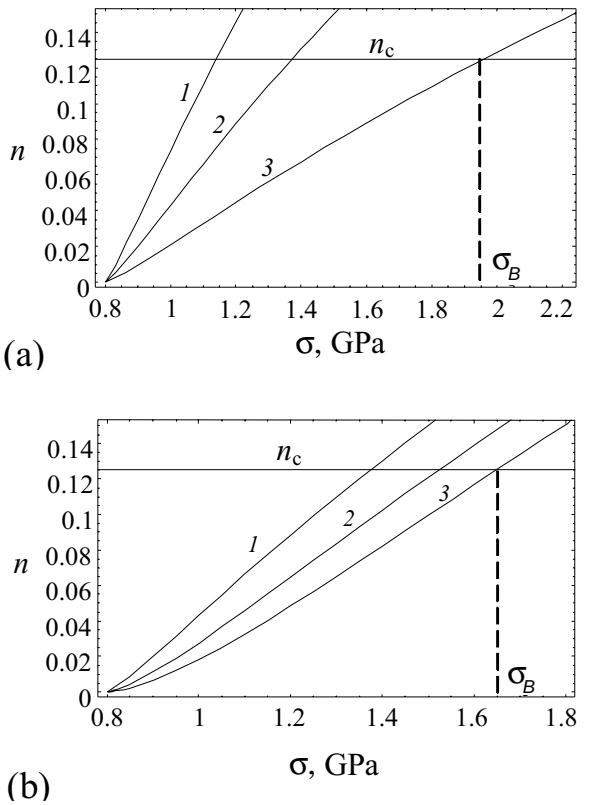

Fig. 4. Dependences of the fraction *n* of the grain boundaries conducting cracks in nanocrystalline Ni on applied tensile stress σ. (a) α=1.5; $\bar{\omega}$=7, 10 and 15° (curves 1, 2, and 3, respectively). (b) ω=10°; α=1.5, 2 and 2.5 (curves 1, 2 and 3, respectively).

on $\bar{\omega}$ as well. In contrast, for a preset applied stress σ, the value of *n* decreases with rising $\bar{\omega}$ (see Fig. 4a). As a result, with an increase in $\bar{\omega}$, the ultimate strength σ_B (determined by the point of the intersection of the corresponding curve $n(\sigma)$ with the horizontal line $n=n_c$) of the nanocrystalline solid also increases. As it follows from Figs. 3b and 4b, an increase in the parameter α (which corresponds to the shrinking of the distribution of disclinations over strengths ω) leads to an increase in both strain-to-failure ε_f and ultimate strength σ_B.

Notice that the value of the ultimate strength σ_B substantially depends on the structure of GBs of the nanocrystalline solid and grows with an increase in the fraction of high-angle GBs. If high-angle GBs dominate in nanocrystalline Ni, then the calculated values of σ_B (see Fig. 4) appear to be higher than the corresponding experimental values. Also, the calculated values of strain-to-failure ε_f in deformed nanocrystalline Ni (17–19%; see Fig. 3) significantly exceed the corresponding experimental values [29]. The possible reasons for the above discrepancies are the absence of the account for stress concentration near nanocrack tips as well as for the presence of the pre-existent, fabrication-produced voids and other imperfections. These factors reduce the values of the critical parameters ε_f and σ_B, in which case they can be close to the corresponding experimentally measured values [29]. At the same time, the above discrepancies show that the strain-to-failure and strength in nanocrystalline materials free from fabrication-produced voids and other imperfections can be larger (or even significantly larger) than those in nanocrystalline materials containing fabrication-produced flaws. As a corollary, one expects that there are perspectives in fabrication of nanocrystalline materials with simultaneously ultra-high strength and good ductility.

5. CONCLUDING REMARKS

Thus, the analysis performed in this paper shows that GB sliding in deformed nanocrystalline materials with finest grains can lead to the generation and subsequent convergence of GB nanocracks. During plastic deformation, the number fraction of GBs containing nanocracks grows, and, when the applied stress and strain reach their critical values, nanocracks converge and form a macrocrack resulting in the catastrophic fracture of the nanocrystalline solid. The critical stress for the brittle fracture of the nanocrystalline solid (ultimate strength) significantly increases with an increase in GB misorientation angles. Therefore, in order to increase the ultimate strength of nanocrystalline solids, it is desired that they primarily contain high-angle GBs with high misorientation angles.

Notice that the calculated values of the ultimate strength σ_B and strain-to-failure ε_f in deformed nanocrystalline Ni (see Figs. 3 and 4) are higher than the corresponding experimental values. The above discrepancies can be in part attributed to reducing both strength σ_B and strain-to-failure ε_f in most of real nanocrystalline materials due to the effects of the pre-existent, fabrication-produced voids and other imperfections. At the same time, the above discrepancies show that the strain-to-failure ε_f and strength σ_B in nanocrystalline materials free from fabrication-produced voids and other imperfections can be larger (or sometimes significantly larger) than those in nanocrystalline materials containing fabrication-produced flaws. In these circumstances, there are perspectives in fabrication of nanocrystalline materials with simultaneously ultra-high strength and good ductility as those free from fabrication-produced flaws. This view is in a good agreement with experimental papers [19–21,45] reporting on fabrication of such nanocrystalline materials.

ACKNOWLEDGEMENTS

The work was supported, in part, by the Russian Federal Agency of Science and Innovations (Contract 02.513.11.3190 of the Program “Industry of Nanosystems and Materials” and grants NSh-2405.2008.1 and MK-1702.2008.1), the Russian Foundation of Basic Research (grant 08-01-00225-a), and Russian Academy of Sciences Program “Structural Mechanics of Materials and Construction Elements”.

REFERENCES

[1] K.S. Kumar, H. Van Swygenhoven and S. Suresh // *Acta Mater.* **51** (2003) 5743.
[2] I.A. Ovid’ko // *Int. Mater. Rev.* **50** (2005) 65.
[3] B.Q. Han, E. Lavernia and F.A. Mohamed // *Rev. Adv. Mater. Sci.* **9** (2005) 1.
[4] D. Wolf, V. Yamakov, S.R. Phillpot, A.K. Mukherjee and H. Gleiter // *Acta Mater.* **53** (2005) 1.
[5] M.A. Meyers, A. Mishra and D.J. Benson // *Progr. Mater. Sci.* **51** (2006) 427.
[6] C.C. Koch // *J. Mater. Sci.* **42** (2007) 1403.
[7] M. Dao, L. Lu, R.J. Asaro, J.T.M. De Hosson and E. Ma // *Acta Mater.* **55** (2007) 4041.
[8] M.Yu. Gutkin and I.A. Ovid’ko, *Plastic Deformation in Nanocrystalline Materials* (Springer, Berlin, 2004).
[9] C.C. Koch, I.A. Ovid’ko, S. Seal and S. Veprek, *Structural Nanocrystalline Materials: Fundamentals and Applications* (Cambridge University Press, Cambridge, 2007).
[10] L.M. Kachanov, *Fundamentals of the theory of plasticity* (Dover Publ., 2004).
[11] G.P. Cherepanov, Mechanics of Brittle Fracture (McGraw-Hill, New York,1979).
[12] A.Yu. *Ishlinskij and* D.D Ivlev, *Mathematical theory of plasticity* (Fizmatlit, Moscow, 2001), In Russian.
[13] N.F. Morozov, *Mathematical problems of the crack theory* (Nauka, Moscow, 1984), In Russian.
[14] Y. Champion, C. Langlois, S. Guerin-Mailly, P. Langlois, J.-L. Bonnentien and M. Hytch // *Science* **300** (2003) 310.
[15] A.A. Karimpoor, U. Erb, K.T. Aust and G. Palumbo // *Scr. Mater.* **49** (2003) 651.
[16] K.S. Kumar, S. Suresh, M.F. Chisholm, J.A. Norton and P. Wang // *Acta Mater.* **51** (2003) 387.
[17] G. He, J. Eckert, W. Loeser and L. Schultz // *Nature Mater.* **2** (2003) 33.
[18] Y.M. Wang and E. Ma // *Acta Mater.* **52** (2004) 1699.
[19] K.M. Youssef, R.O. Scattergood, K.L. Murty and C.C. Koch // *Appl. Phys. Lett.* **85** (2004) 929.
[20] K.M. Youssef, R.O. Scattergood K.L. Murty, J.A. Horton and C.C. Koch // *Appl. Phys. Lett.* **87** (2005) 091904.
[21] K.M. Youssef, R.O. Scattergood, K.L. Murty and C.C. Koch // *Scr. Mater.* **54** (2006) 251.

[22] S.X. McFadden, R.S. Misra, R.Z. Valiev, A.P. Zhilyaev and A.K. Mukherjee // *Nature* **398** (1999) 684.
[23] R.S. Mishra, R.Z. Valiev, S.X. McFadden, R.K. Islamgaliev and A.K. Mukherjee // *Phil. Mag.* A **81** (2001) 37.
[24] A.K. Mukherjee // *Mater. Sci. Eng.* A **322** (2002) 1.
[25] G.-D. Zhan, J.E. Garay and A.K. Mukherjee // *Nano Lett.* **5** (2005) 2593.
[26] X. Zhou, D.M. Hilbert, J.D. Kunz, R.K. Sadagi, V. Shukla, B.H. Kear and A.K. Mukherjee // *Mater. Sci. Eng.* A **394** (2005) 353.
[27] X. Xu, T. Nishimura, N. Hirosaki, R.J. Xie, Y. Yamamoto and H. Tanaka // *Acta Mater.* **54** (2006) 255.
[28] R.C. Hugo, H. Kung, J.R. Weertman, R. Mitra, J.A. Knapp and D.M. Follstaedt // *Acta Mater.* **51** (2003) 1937.
[29] H. Li and F. Ebrahimi // *Appl. Phys. Lett.* **84** (2004) 4307.
[30] H. Li and F. Ebrahimi // *Adv. Mater.* **17** (2005) 1969.
[31] F. Ebrahimi, A.J. Liscano, D. Kong, Q. Zhai and H. Li // *Rev. Adv. Mater. Sci.* **13** (2006) 33.
[32] D. Farkas, H. Van Swygenhoven and P.M. Derlet // *Phys. Rev.* B **66** (2002) 060101 (R).
[33] H. Van Swygenhoven, P.M. Derlet, A. Hasnaoui and M. Samaras, In: *Nanostructures: Synthesis, Functional Properties and Applications*, ed. by T. Tsakalakos, I.A. Ovid'ko and A.K. Vasudevan (Kluwer, Dordrecht, 2003), p. 155.
[34] D. Farkas, S. Van Petegem, P.M. Derlet and H. Van Swygenhoven // *Acta Mater.* **53** (2005) 3115.
[35] Y. Mo and I. Szlufarska // *Appl. Phys. Lett.* **90** (2007) 181926.
[36] N.F. Morozov, I.A. Ovid'ko, Yu.V. Petrov and A.G. Sheinerman // *Rev. Adv. Mater. Sci.* **4** (2003) 65.
[37] N.F. Morozov, I.A. Ovid'ko, Yu.V. Petrov and A.G. Sheinerman // *Doklady Physics* **51** (2006) 69.
[38] I.A. Ovid'ko and A.G. Sheinerman // *Acta Mater.* **52** (2004) 1201.
[39] I.A. Ovid'ko and A.G. Sheinerman // *Acta Mater.* **53** (2005) 1347.
[40] V.A. Pozdnyakov and A.M. Glezer // *Phys. Solid State* **47** (2005) 817.
[41] S.V. Bobylev, N.F. Morozov and I. A. Ovidko // *Phys. Solid State* **49** (2007) 1098.
[42] I.A. Ovid'ko and A.G. Sheinerman // *Appl. Phys. Lett.* **90** (2007) 171927.
[43] I.A. Ovid'ko and A.G. Sheinerman // *Phys. Solid State* **50** (2008) 1111.
[44] I.A. Ovid'ko // *J. Mater. Sci.* **42** (2007) 1694.
[45] I.A. Ovid'ko and A.G. Sheinerman // *Phys. Rev.* B **77** (2008) 054109.
[46] A.E. Romanov and V.I. Vladimirov, In: *Dislocations in Solids*, ed. by F.R.N. Nabarro (North-Holland, Amsterdam, 1992), Vol. 9, p. 191.
[47] J. Ziman // *Models of Disorder* (Cambridge University Press, Cambridge, 1979).
[48] J.P. Clerc, G. Giraud, J.M. Laugier and J.M. Lucks // *Adv. Phys.* **39** (1990) 191.
[49] D. Stauffer and A. Aharony, *Introduction to Percolation Theory* (Taylor and Francis, London, 1992).
[50] M. Sahimi, *Applications of Percolation Theory* (Taylor and Francis, London, 1994).
[51] I.A. Ovid'ko and A.G. Sheinerman // *Acta Mater.* (2009), in press.
[52] L.D. Landau and E.M. Lifshitz, *Statistical Physics*. *Part 1* (Pergamon, 1980).
[53] C.J. Smithells and E.A. Brands, *Metals Reference Book* (Butterworth, London, 1976).